ChemComm

COMMUNICATION

View Article Online
View Journal | View Issue

Cite this: *Chem. Commun.*, 2019, **55**, 3895

Received 11th January 2019,
Accepted 5th March 2019

DOI: 10.1039/c9cc00278b

rsc.li/chemcomm

A gene-targeted polymerase-mediated strategy to identify O^6-methylguanine damage†

Claudia M. N. Aloisi, Shana J. Sturla and Hailey L. Gahlon *

Detecting DNA adducts in cancer genes is important for understanding cancer etiology. This study reports a strategy to identify the mutagenic DNA adduct O^6-methylguanine in K-Ras. The strategy involves selective replication past a synthetic primer when placed opposite O^6-methylguanine. Future work can apply this approach to other cancer-relevant genes.

DNA adducts contribute to cancer initiation and can be biomarkers of carcinogenesis as well as cancer therapy efficacy. Strategies to detect DNA damage often describe global damage levels, *e.g.* mass spectrometry, immunological assays and ^{32}P-postlabeling, and information regarding their genomic sequence context is missing.[1–5] In recent years, various methods have been developed to report on damage in a sequence-specific context, for instance single-molecule approaches like nanopore and SMRT sequencing as well as whole genome sequencing.[6–14] Recently, the emergence of epigenetic factors being important in driving biological responses to chemicals[15,16] emphasizes the need for methods to define the presence of DNA damage in particular genes. However, DNA damage sequencing approaches are only recently emerging and have not been generalized to many forms of DNA damage. O^6-Methylguanine (O^6-MeG) is a mutagenic DNA adduct that is formed upon exposure to endogenous and exogenous alkylating agents, *e.g. N*-nitroso-*N*-methylurea and *N*-nitrosodimethylamine.[17,18] The K-Ras gene is mutated in 43% of colon cancer cases,[19] for which nitrosamine exposure may be a contributing factor, but lack of strategies to investigate the formation of O^6-MeG in K-Ras and mutation hotspot loci limits the capacity to relate mutagenesis with specific DNA methylation events. This work describes a proof of principle approach to detect the mutagenic adduct O^6-MeG in the K-Ras gene sequence.

In previous studies addressing structural requirements for extension from a modified primer terminus, we reported that Dpo4, a Y-family DNA polymerase, elongated past O^6-alkylguanine DNA adducts when paired opposite a synthetic nucleoside analogue.[20,21] This process was effective for elongation past O^6-MeG when paired opposite the hydrophobic nucleoside analogue Benzi, designed to pair preferentially opposite O^6-alkylguanines.[20–23] When Benzi was paired opposite G, however, Dpo4 stalled and the primer was not elongated.[21] We envisioned that the selective extension past O^6-MeG as compared to G could be the basis of a strategy to detect O^6-MeG. However, preliminary studies with oligonucleotides in the K-Ras sequence (Table 1) revealed that Dpo4 elongated past Benzi paired opposite both O^6-MeG and G similarly (Fig. S4, ESI†). On the other hand, replacing Dpo4 with either KlenTaq or a previously reported mutant of KlenTaq M474K showed selective extension, *i.e.* Benzi primer was only enzymatically elongated when paired opposite O^6-MeG and not G (Fig. 1 and Fig. S6, ESI†). In this study, we have developed a strategy to detect O^6-MeG in the target gene sequence of K-Ras by using a 3′-Benzi-modified primer that hybridizes opposite damaged and undamaged templates and an engineered DNA polymerase that is selective and efficient for extension of modified primers (Scheme 1).

The potential of selective enzymatic extension past O^6-MeG in a target gene was tested in the sequence of codon 12 of the K-Ras gene, a mutational hotspot locus that is frequently mutated in colorectal cancers.[19] We performed primer extension experiments with 3′-Benzi-modified primers and templates with the sequence of K-Ras gene where the second base of codon 12 contains a G or O^6-MeG (Table 1). Dpo4 elongated past Benzi paired opposite both O^6-MeG and G similarly, suggesting a gap in the potential to extend the strategy to other gene-related sequences (Fig. S4, ESI†).

Table 1 Sequences for DNA templates and primers

Name	DNA sequence (5′–3′)[a]
G template	GTA GTT GGA GCT GGT GGC GTA GGC AAG
O^6-MeG template	GTA GTT GGA GCT GG*T GGC GTA GGC AAG
Benzi primer 1	CTT GCC TAC GCC AP
Benzi primer 2	NCTT GCC TAC GCC AP

[a] G* = O^6-MeG, underlined bases = codon 12 of K-Ras, P = Benzi, N = $(T)_{21}$ that is represented as a 5′-overhang (green line) in Scheme 1A.

Department of Health Sciences and Technology, ETH Zürich, Schmelzbergstrasse 9, 8092 Zürich, Switzerland. E-mail: hailey.gahlon@hest.ethz.ch

† Electronic supplementary information (ESI) available. See DOI: 10.1039/c9cc00278b

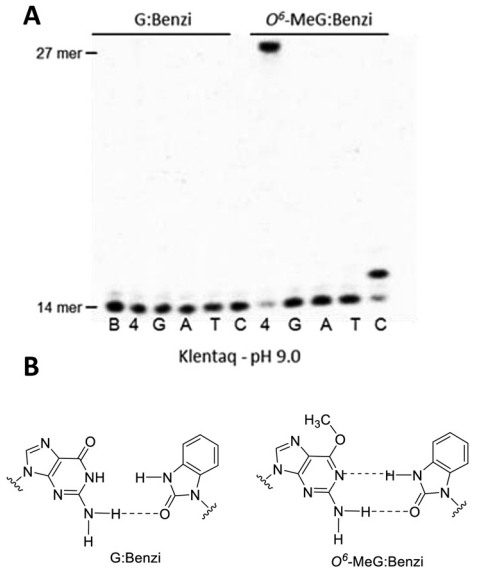

Fig. 1 (A) KlenTaq-mediated elongation past G:Benzi (left) and O^6-MeG:Benzi (right) at 55 °C for 10 min at pH 9.0 (lanes in the gel are designated as follows: B = 14 mer blank, 4 = all 4 canonical dNTPs, and the single nucleotide conditions include: G = only dGTP, A = only dATP, T = only dTTP, and C = only dCTP). (B) Proposed base pairing interactions for Benzi opposite G and O^6-MeG.

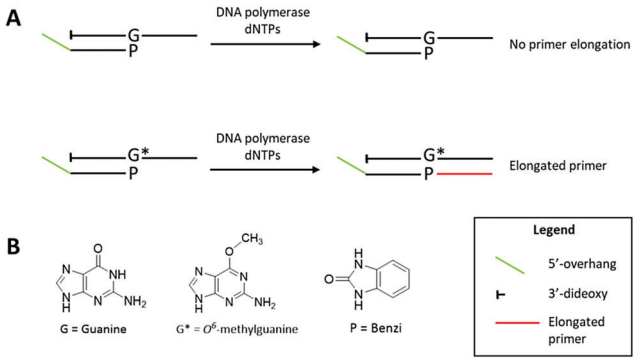

Scheme 1 (A) KlenTaq elongates specifically past O^6-MeG:Benzi termini and does not elongate past G:Benzi in the K-Ras gene sequence. This discrimination provides a mean to detect O^6-MeG by linear DNA amplification. Extension products are separated by polyacrylamide gel electrophoresis and visualized by SYBR Gold staining. The elongated primer (red region) is distinguishable from the O^6-MeG- and G-containing templates by the presence of a 5′ overhang (green region) on the primer. The template contains a 3′-dideoxy modification to prevent undesired extension of the template. (B) Chemical structures of guanine (G), O^6-MeG (G*) and Benzi (P).

We tested the influence of the enzyme on this process, replacing Dpo4 with bypass-proficient engineered enzymes, KlenTaq and its M747K mutant.[23,24] The change in the enzyme resulted in selective extension, whereby Benzi primer was only enzymatically elongated when paired opposite O^6-MeG but not G (Fig. 1 and Fig. S6, ESI†).

The ability for extension by KlenTaq past Benzi-containing primers paired opposite G and O^6-MeG was evaluated by further primer extension analysis. KlenTaq elongated selectively past Benzi paired opposite O^6-MeG, and not G, in the K-Ras DNA sequence (Table 1). For these experiments, KlenTaq DNA polymerase (25 units), DNA (10 nM) and dNTPs (10 μM) were incubated at 55 °C for 10 min. For O^6-MeG:Benzi DNA, KlenTaq extended in an error-free manner and only dCTP was inserted under single nucleotide conditions (Fig. 1). In the case of all four dNTPs, KlenTaq performed full-length extension for O^6-MeG:Benzi and no extension was observed for G:Benzi. KlenTaq efficiently elongated past O^6-MeG:Benzi DNA in the presence of all four dNTPs (90% elongation, Fig. 1A). Analogous primer extension assays were performed with a lower concentration of KlenTaq (2.5 units) and less elongation was observed for the O^6-MeG:Benzi DNA (~65% extension, Fig. S5, ESI†).

Elongation past Benzi-containing DNA was also tested with the KlenTaq mutant M747K, reported to have an increased proclivity for lesion bypass. This engineered polymerase is thought to increase favourable electrostatic interactions between the DNA backbone and the enzyme, thus promoting damage bypass.[25,26] For the primer extension reactions, KlenTaq M747K (20 nM), DNA (10 nM) and dNTPs (10 μM) were incubated at 55 °C for 10 min (Fig. S6, ESI†). For G:Benzi DNA, KlenTaq M747K did not catalyze DNA synthesis (Fig. S6, ESI†). Conversely, for O^6-MeG:Benzi DNA, KlenTaq M747K elongated by correctly inserting dCMP (Fig. S6, ESI†). Also, for O^6-MeG:Benzi, KlenTaq M747K elongated the primer to the full length of the template in the presence of all 4 dNTPs (~100%, Fig. S6, ESI†). KlenTaq M747K-mediated elongation was also tested at 72 °C, however, no full-length extension products were observed for either G:Benzi or O^6-MeG:Benzi (Fig. S7, ESI†). A small percentage of dCMP (~10%) was inserted for O^6-MeG:Benzi (Fig. S7, ESI†). It is likely that at 72 °C the DNA is not hybridized, as the theoretical T_m is ~50 °C. Therefore, temperatures below 72 °C are necessary for optimal DNA polymerase-mediated elongation. A slight reduction in selectivity past O^6-MeG:Benzi *vs.* G:Benzi was observed for KlenTaq M747K (Fig. S6, ESI†) compared to wild type KlenTaq (Fig. 1). Therefore, wild type KlenTaq was used in further experiments.

Having established wild type KlenTaq as the preferred enzyme for selective extension from DNA templates containing O^6-MeG, we tested if the Benzi primer could be linearly amplified in the presence of G and O^6-MeG templates. For these studies, a modified Benzi oligonucleotide (Benzi primer 2, Table 1) was synthesized (Fig. S3, ESI†) with a 21 nt 5′-overhang to enable resolution of amplicons (48 nt extended primer) from the initial template (27 nt). To ensure that the observed 48 nt oligo signal was exclusively a result of elongation of the Benzi primer, templates with the 3′-dideoxy ends were used. To achieve the highest selectivity and enzyme efficiency, we optimized temperature and time of each reaction step, cycle number, concentration of primer and templates. In addition, we evaluated the effect of varying concentrations of Mg^{2+} ions (Fig. S8, ESI†). Final conditions for the amplification reactions consisted of Benzi primer 2 (200 nM) incubated with either O^6-MeG or G template (2 nM each template), KlenTaq (20 nM) and all four dNTPs (250 μM). Alternating cycles (35) of DNA melting (95 °C, 30 s), annealing (40 °C, 30 s) and extension step (55 °C, 30 s) were performed and products were separated on polyacrylamide gels and visualized by staining with SYBR gold. Under these linear amplification conditions,

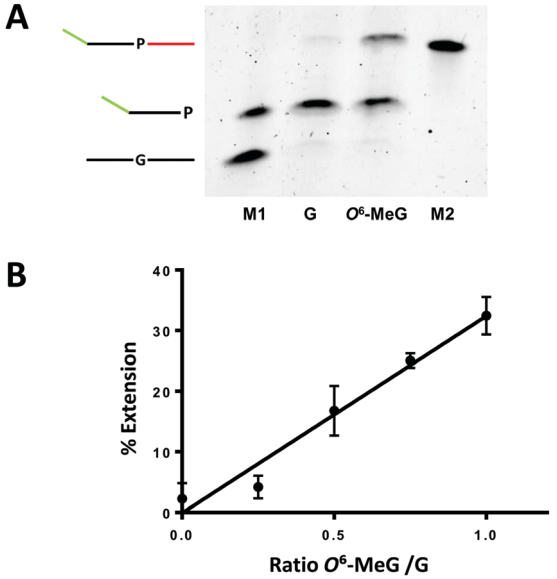

Fig. 2 KlenTaq-mediated elongation past G:Benzi and O^6-MeG:Benzi with Benzi primer 2 (Table 1). Linear amplification conditions comprised of (1) denaturation at 95 °C for 2 min; (2) 35 cycles alternating steps of denaturation at 95 °C for 30 s, annealing at 40 °C for 30 s, extension at 55 °C for 30 s; (3) final extension at 55 °C for 3 min; pH 9, 1XKTQ buffer. (A) Gel separated amplicons (M1 = marker lane with 27 mer G template and 35 mer Benzi primer 2; G = reaction with G template; O^6-MeG = reaction with O^6-MeG template; M2 = marker lane with 48 mer extended primer). Note: initial templates are not detected by SYBR Gold staining as they are below the limit of detection. (B) Linear amplification was performed in the presence of G and O^6-MeG templates with increasing concentrations of O^6-MeG template and a constant concentration of G template (2 nM). All reactions were performed in three independent technical replicates ($y = 32.49x - 0.11$; $R^2 = 0.97$).

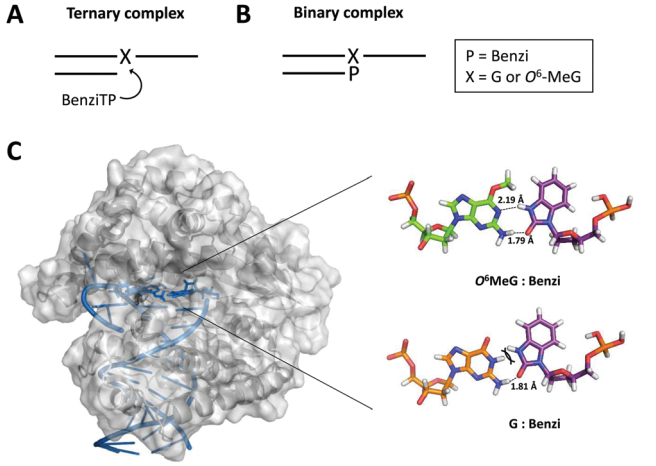

Fig. 3 (A) Scheme of the ternary complex previously crystallized for X-ray analysis (X = G or O^6-MeG). (B) Scheme of the binary complex with Benzi covalently bound to the 3′ end of the primer (P = Benzi). (C) KlenTaq (PDB ID: 3RTV) was energy minimized with Molecular Operating Environment software. The active site of KlenTaq (zoomed-in region) shows Benzi paired opposite O^6-MeG (top) and G (bottom). Two hydrogen bond interactions were computed for O^6-MeG:Benzi and one hydrogen bond for G:Benzi.

selective elongation for O^6-MeG:Benzi DNA was observed (Fig. 2A), corroborating findings from the primer extension data (Fig. 1).

To test if the selective elongation from O^6-MeG:Benzi could be a viable strategy for identifying O^6-MeG, we performed linear amplification studies in a mixture of damaged and undamaged DNA. Here, the concentration of G template was constant (2 nM) while increasing the concentrations of O^6-MeG (0, 0.5, 1, 1.5, 2 nM). In the presence of a mixture of DNA templates, the signal increased as a function of increasing concentrations of O^6-MeG (Fig. 2B). The ratio of O^6-MeG to G plotted against the corresponding amount of extension showed a linear relationship (Fig. 2B). In a 50 : 50 mixture of O^6-MeG : G, 15% of extension was observed and extension doubled (30%) with a 2-fold increase in the ratio of O^6-MeG:G. These results demonstrate Benzi as an effective chemical marker to detect O^6-MeG in a mixture of undamaged and damaged DNA.

To understand structural interactions that contribute to the preferred extension of Benzi paired opposite O^6-MeG by KlenTaq, we performed computational modelling studies. Previous X-ray data with Benzi as an incoming triphosphate (BenziTP) paired opposite O^6-MeG (*i.e.* ternary complex; Fig. 3A) showed BenziTP pairs opposite O^6-MeG with two hydrogen bond interactions.[26] Starting from the ternary complex crystal structure (PDB ID: 3RTV)[26] with wild type KlenTaq, undamaged primer:template DNA, and an incoming dCTP we (1) removed the incoming dCTP (2) replaced the terminal 3′ nucleotide on the primer strand with Benzi, and (3) inserted G and O^6-MeG in the template (Fig. 3B) to reflect the configuration of the experiments described above.

We evaluated the distance and orientation of the terminal base pairs in the active site of KlenTaq. First, we compared deoxyribose distances for O^6-MeG:Benzi and the natural G:C base pairs. We found that the C1′–C1′ distance for the G:C base pair (10.5 Å) is comparable to the O^6-MeG:Benzi base pair (10.4 Å and 10.2 Å for the methyl group in a distal and proximal conformation, respectively, Fig. S9, ESI†). These distances are similar to what was reported for the X-ray structure; O^6-MeG:Benzi with a slightly longer C1′–C1′ distance of 11.0 Å and G:C of 10.6 Å.[26] We speculate that the closer distance of O^6-MeG:Benzi in our modelled data may result from the slight torsion that Benzi imposes when covalently bound to the DNA primer (binary complex, Fig. 3B). Next, we compared the orientation of Benzi in the enzymatic pocket when paired opposite O^6-MeG and G. We observed minor rotations on amino acid residues; however, the overall orientation of Benzi was not sufficiently different when paired opposite damaged and undamaged DNA.

Overall energies and hydrogen bond interactions were determined for terminal base pairs in the active site of KlenTaq. We determined the computed energies of the terminal O^6-MeG:Benzi and G:Benzi base pairs. These calculated energies take into account both van der Waals and hydrogen bond interactions. Computed energies of −0.3 kcal mol^{-1} for O^6-MeG:Benzi and +26 kcal mol^{-1} for G:Benzi were determined. Further, we found that the hydrogen bond pattern in our model corroborates the previous X-ray data.[26] For example, Benzi and O^6-MeG interact by two hydrogen bonds; one hydrogen bond between the N1 on O^6-MeG and the –NH donor on Benzi (2.19 Å, Fig. 3C) and

another between the NH_2 donor on O^6-MeG and the carbonyl group on Benzi (1.79 Å when the methyl group is in the distal conformation, Fig. 3C; 1.96 Å in the proximal conformation, Fig. S9, ESI†). Further, G:Benzi displays a potential steric clash between the –NH moiety on Benzi and the –NH at the N1 position on G (Fig. 3C), possibly impeding KlenTaq catalysis. On the contrary, O^6-MeG:Benzi is more analogous to the natural G:C Watson–Crick base pair, but with two hydrogen bonds. This more favourable configuration of O^6-MeG:Benzi *vs.* G:Benzi may explain the observed preferential elongation by KlenTaq.

In conclusion, this work presents a first enzyme-based strategy reporting on the presence of O^6-MeG in the cancer-relevant gene sequence of K-Ras by means of synthetic DNA-based amplification. This strategy works by identifying O^6-MeG in a sequence-specific manner and, therefore, could be useful for linking modifications in particular genes with specific mutational outcomes, which is not possible using typical DNA adduct detection methods that generally lose information about adduct sequence. In this strategy, damage is detected in a pre-defined locus. Compared to genome-wide damage mapping strategies, this approach provides a targeted strategy that could be adapted to other cancer genes, thereby providing defined chemical resolution of damage in hotspot regions of genes. Future work will require assessing adduct selectivity, as well as addressing the need for increased sensitivity to detect damage at biologically relevant levels, which would require a companion enrichment strategy to assess low abundance forms of damage. Furthermore, this approach could be expanded to detect O^6-MeG in other cancer-relevant gene sequences, thereby leading to a better understanding of the relationship between DNA damage and disease initiation and progression.

We acknowledge the Swiss National Science Foundation (31003A_156280), the European Research Council (260341) and the ETH Career Seed Grant (SEED-16 18-1).

Conflicts of interest

There are no conflicts to declare.

References

1 J. Guo, P. W. Villalta and R. J. Turesky, *Anal. Chem.*, 2017, **89**, 11728–11736.
2 R. Singh and P. B. Farmer, *Carcinogenesis*, 2006, **27**, 178–196.
3 K. Brown, *Methods Mol. Biol.*, 2012, **817**, 207–230.
4 N. J. Jones, *Methods Mol. Biol.*, 2012, **817**, 183–206.
5 D. H. Phillips, P. B. Farmer, F. A. Beland, R. G. Nath, M. C. Poirier, M. V. Reddy and K. W. Turteltaub, *Environ. Mol. Mutagen.*, 2000, **35**, 222–233.
6 J. Hu, S. Adar, C. P. Selby, J. D. Lieb and A. Sancar, *Genes Dev.*, 2015, **29**, 948–960.
7 W. Li, J. Hu, O. Adebali, S. Adar, Y. Yang, Y.-Y. Chiou and A. Sancar, *Proc. Natl. Acad. Sci. U. S. A.*, 2017, **114**, 6752–6757.
8 J. Wu, M. McKeague and S. J. Sturla, *J. Am. Chem. Soc.*, 2018, **140**, 9783–9787.
9 J. Ding, M. S. Taylor, A. P. Jackson and M. A. M. Reijns, *Nat. Protoc.*, 2015, **10**, 1433.
10 J. Hu, J. D. Lieb, A. Sancar and S. Adar, *Proc. Natl. Acad. Sci. U. S. A.*, 2016, **113**, 11507.
11 N. An, A. M. Fleming, H. S. White and C. J. Burrows, *ACS Nano*, 2015, **9**, 4296–4307.
12 I. A. Trantakis, A. Nilforoushan, H. A. Dahlmann, C. K. Stäuble and S. J. Sturla, *J. Am. Chem. Soc.*, 2016, **138**, 8497–8504.
13 J. Hu, O. Adebali, S. Adar and A. Sancar, *Proc. Natl. Acad. Sci. U. S. A.*, 2017, **114**, 6758–6763.
14 B. A. Flusberg, D. R. Webster, J. H. Lee, K. J. Travers, E. C. Olivares, T. A. Clark, J. Korlach and S. W. Turner, *Nat. Methods*, 2010, **7**, 461.
15 A. M. Fleming, Y. Ding and C. J. Burrows, *Proc. Natl. Acad. Sci. U. S. A.*, 2017, **114**, 2604–2609.
16 G. P. Pfeifer, *Int. J. Mol. Sci.*, 2018, **19**, 1166.
17 A. J. Likhachev, M. N. Ivanov, H. Bresil, G. Planche-Martel, R. Montesano and G. P. Margison, *Cancer Res.*, 1983, **43**, 829–833.
18 S. Arimoto-Kobayashi, K. Kaji, G. M. A. Sweetman and H. Hayatsu, *Carcinogenesis*, 1997, **18**, 2429–2433.
19 R. P. Jones, P. A. Sutton, J. P. Evans, R. Clifford, A. McAvoy, J. Lewis, A. Rousseau, R. Mountford, D. McWhirter and H. Z. Malik, *Br. J. Cancer*, 2017, **116**, 923–929.
20 H. L. Gahlon, B. W. Schweizer and S. J. Sturla, *J. Am. Chem. Soc.*, 2013, **135**, 6384–6387.
21 H. L. Gahlon, M. L. Boby and S. J. Sturla, *ACS Chem. Biol.*, 2014, **9**, 2807–2814.
22 H. L. Gahlon and S. J. Sturla, *Chem. – Eur. J.*, 2013, **19**, 11062–11067.
23 L. A. Wyss, A. Nilforoushan, D. M. Williams, A. Marx and S. J. Sturla, *Nucleic Acids Res.*, 2016, **44**, 6564–6573.
24 S. Obeid, A. Schnur, C. Gloeckner, N. Blatter, W. Welte, K. Diederichs and A. Marx, *ChemBioChem*, 2011, **12**, 1574–1580.
25 C. Gloeckner, K. B. M. Sauter and A. Marx, *Angew. Chem., Int. Ed.*, 2007, **46**, 3115–3117.
26 K. Betz, A. Nilforoushan, L. A. Wyss, K. Diederichs, S. J. Sturla and A. Marx, *Chem. Commun.*, 2017, **53**, 12704–12707.

